Two-photon excitation STED microscopy

Gael Moneron and Stefan W. Hell*

Department of NanoBiophotonics, Max Planck Institute for Biophysical Chemistry, Am Fassberg 11, 37077 Göttingen, Germany
**shell@gwdg.de*

Abstract: We report sub-diffraction resolution in two-photon excitation (TPE) fluorescence microscopy achieved by merging this technique with stimulated-emission depletion (STED). We demonstrate an easy-to-implement and promising laser combination based on a short-pulse laser source for two-photon excitation and a continuous-wave (CW) laser source for resolution enhancement. Images of fluorescent nanoparticles and the immunostained transcription regulator NFκB in mammalian cell nuclei exhibit resolutions of <50 nm and ~70 nm in the focal plane, respectively, corresponding to a 4–5.4-fold improvement over the diffraction barrier.

OCIS codes: (180.1790) Confocal microscopy; (180.2520) Fluorescence microscopy; (180.4315) Nonlinear microscopy; (180.5810) Scanning microscopy; (180.6900) Three-dimensional microscopy; (110.0180) Microscopy.

References and links

1. W. Denk, J. H. Strickler, and W. W. Webb, "Two-photon laser scanning fluorescence microscopy," Science **248**(4951), 73–76 (1990).
2. S. W. Hell, and J. Wichmann, "Breaking the diffraction resolution limit by stimulated emission: stimulated emission depletion microscopy," Opt. Lett. **19**(11), 780–782 (1994).
3. F. Helmchen, and W. Denk, "Deep tissue two-photon microscopy," Nat. Methods **2**(12), 932–940 (2005).
4. A. Diaspro, G. Chirico, and M. Collini, "Two-photon fluorescence excitation and related techniques in biological microscopy," Q. Rev. Biophys. **38**(02), 97–166 (2005).
5. K. Svoboda, and R. Yasuda, "Principles of two-photon excitation microscopy and its applications to neuroscience," Neuron **50**(6), 823–839 (2006).
6. S. W. Hell, "Microscopy and its focal switch," Nat. Methods **6**(1), 24–32 (2009).
7. T. A. Klar, and S. W. Hell, "Subdiffraction resolution in far-field fluorescence microscopy," Opt. Lett. **24**(14), 954–956 (1999).
8. V. Westphal, and S. W. Hell, "Nanoscale resolution in the focal plane of an optical microscope," Phys. Rev. Lett. **94**(14), 143903 (2005).
9. G. Donnert, J. Keller, R. Medda, M. A. Andrei, S. O. Rizzoli, R. Lührmann, R. Jahn, C. Eggeling, and S. W. Hell, "Macromolecular-scale resolution in biological fluorescence microscopy," Proc. Natl. Acad. Sci. U.S.A. **103**(31), 11440–11445 (2006).
10. B. Harke, J. Keller, C. K. Ullal, V. Westphal, A. Schönle, and S. W. Hell, "Resolution scaling in STED microscopy," Opt. Express **16**(6), 4154–4162 (2008).
11. E. Rittweger, K. Y. Han, S. E. Irvine, C. Eggeling, and S. W. Hell, "STED microscopy reveals crystal colour centres with nanometric resolution," Nat. Photonics **3**(3), 144–147 (2009).
12. K. I. Willig, S. O. Rizzoli, V. Westphal, R. Jahn, and S. W. Hell, "STED microscopy reveals that synaptotagmin remains clustered after synaptic vesicle exocytosis," Nature **440**(7086), 935–939 (2006).
13. R. R. Kellner, C. J. Baier, K. I. Willig, S. W. Hell, and F. J. Barrantes, "Nanoscale organization of nicotinic acetylcholine receptors revealed by stimulated emission depletion microscopy," Neuroscience **144**(1), 135–143 (2007).
14. U. V. Nägerl, K. I. Willig, B. Hein, S. W. Hell, and T. Bonhoeffer, "Live-cell imaging of dendritic spines by STED microscopy," Proc. Natl. Acad. Sci. U.S.A. **105**(48), 18982–18987 (2008).
15. V. Westphal, S. O. Rizzoli, M. A. Lauterbach, D. Kamin, R. Jahn, and S. W. Hell, "Video-rate far-field optical nanoscopy dissects synaptic vesicle movement," Science **320**(5873), 246–249 (2008).
16. List of fluorescent dyes used in STED microscopy: *http://www.mpibpc.mpg.de/abteilungen/200/STED_Dyes.htm*
17. D. Wildanger, E. Rittweger, L. Kastrup, and S. W. Hell, "STED microscopy with a supercontinuum laser source," Opt. Express **16**(13), 9614–9621 (2008).
18. B. R. Rankin, R. R. Kellner, and S. W. Hell, "Stimulated-emission-depletion microscopy with a multicolor stimulated-Raman-scattering light source," Opt. Lett. **33**(21), 2491–2493 (2008).
19. K. I. Willig, B. Harke, R. Medda, and S. W. Hell, "STED microscopy with continuous wave beams," Nat. Methods **4**(11), 915–918 (2007).

#113468 - $15.00 USD Received 26 Jun 2009; revised 29 Jul 2009; accepted 31 Jul 2009; published 3 Aug 2009

20. S. W. Hell, M. Booth, S. Wilms, C. M. Schnetter, A. K. Kirsch, D. J. Arndt-Jovin, and T. M. Jovin, "Two-photon near- and far-field fluorescence microscopy with continuous-wave excitation," Opt. Lett. **23**(15), 1238–1240 (1998).
21. M. J. Booth, and S. W. Hell, "Continuous wave excitation two-photon fluorescence microscopy exemplified with the 647-nm ArKr laser line," J. Microsc. **190**(3), 298–304 (1998).
22. T. Staudt, M. C. Lang, R. Medda, J. Engelhardt, and S. W. Hell, "2,2′-thiodiethanol: a new water soluble mounting medium for high resolution optical microscopy," Microsc. Res. Tech. **70**(1), 1–9 (2007).

1. Introduction

Far-field fluorescence microscopy is by far the most commonly used microscopy technique for biological investigations due to the non-invasiveness of focused light and the high molecular specificity of fluorescent labeling. Among the noteworthy developments that have been made in this field during the past two decades, one can cite the implementation of two-photon excitation (TPE) [1] and the breaking of the diffraction resolution barrier with stimulated-emission depletion (STED) [2]. Although their combination should be possible, these two microscopy techniques have so far not been merged. Here, we demonstrate an easy-to-implement experimental configuration for overcoming the resolution limits of TPE microscopy with STED.

TPE fluorescence microscopy is well-established for three-dimensional (3D) imaging of biological samples ranging from cellular membranes to millimeter-thick brain slices. Detailed descriptions of theory, implementation and applications of TPE microscopy can be found in numerous excellent reviews [3–5]. Briefly, a fluorophore emits fluorescence light after it has been raised to its first excited singlet state by the simultaneous absorption of two photons bridging the energy gap between the excited state and the ground state. Effective quasi-simultaneous absorption of two photons necessitates a high temporal and spatial photon density, facilitated by high peak-power laser pulses. Since the advent of solid state mode-locked laser sources this requirement has been easily met and extensively exploited in fluorescence microscopy.

TPE offers several advantages over single-photon excitation (SPE). Owing to the quadratic dependence of the excitation efficiency with the intensity of excitation light, the volume of fluorescence emission is largely restricted to the region of the focal diffraction main maximum. Unlike with SPE, virtually no out-of-focus fluorescence is generated, resulting in the intrinsic ability of TPE to perform optical sectioning in scanning microscopy. The confinement of TPE restricts photobleaching and phototoxicity to the focal area, although photobleaching tends to occur faster in the focal region under TPE than under SPE. The use of photons of longer wavelength, typically in the near-infrared (NIR), also helps to reduce the overall photodamage and permits a deeper penetration in scattering tissue. However, since it relies on focusing, the resolution of TPE microscopy is restricted by the diffraction-limited spatial extent of the probing volume. In fact, the resolution is typically ~30% poorer than the SPE equivalent, because the reduction of the full-width-half-maximum (FWHM) of the excitation volume resulting from the quadratic dependence of the excitation does not fully compensate for the requirement of a longer excitation wavelength.

In parallel to the development of TPE microscopy, far-field optical techniques have emerged for breaking the diffraction-limited resolution-barrier given by $d \approx \lambda/(2NA)$, where λ is the wavelength of light and *NA* the numerical aperture of the objective lens. Viewed from a general perspective, all these fluorescence 'nanoscopy' techniques exploit a (light-induced) transition between a fluorescent state and a dark state [6] in order to switch on or off the ability of the fluorophore to fluoresce. STED microscopy has proven to be a particularly powerful approach [7–11] for overcoming the diffraction barrier and has been applied to important biological questions [12–15] that were inaccessible to other techniques. In a typical STED microscope, the fluorescence ability of dye molecules located in the outer part of the diffraction-limited excitation area is transiently inhibited so that only fluorophores from the central part of the diffraction limited excitation spot are able to emit spontaneously. The physical process used for this reversible inhibition of fluorescence is stimulated emission. Stimulated emission instantly returns an excited molecule to the ground state by forcing it to

#113468 - $15.00 USD Received 26 Jun 2009; revised 29 Jul 2009; accepted 31 Jul 2009; published 3 Aug 2009

emit a photon identical to the one used to induce the transition, making fluorescence impossible or at least improbable. The stimulated photons are not detected in this case as the wavelength used for stimulated emission is red-shifted with respect to the fluorescence detection window. Squeezing the focal volume of fluorescence signaling is in practice achieved by overlapping the spot of excitation light with a spot of light for STED featuring an intensity zero; usually a doughnut-shaped spot featuring a central deep minimum. The resulting resolution is then not fundamentally limited by the wave nature of light but instead depends on the efficiency of the light-driven depletion of the excited state population; it obeys the formula $d_{STED} \approx \lambda \Big/ \left(2NA\sqrt{1+I/I_S} \right)$ where I is the intensity at the maximum of the STED doughnut and I_S a saturation intensity [8,10] which scales linearly with the inverse of the cross-section for stimulated emission at the used wavelength. Requiring just a single photon, stimulated emission *per se* is a linear optical process.

In order to reach a high depletion efficiency the excitation cross-section of the fluorophore should be negligible at the STED wavelength. A large number of fluorophore-wavelength pairs covering the visible and NIR range of the spectrum have been used for STED [16]. In the NIR, Ti:Sapphire lasers are very convenient sources for providing the STED beam, while optical parametric oscillators (OPO) or optical parametric amplifiers (OPA) have been the most obvious sources in the visible range. Recent developments in laser technologies offering multicolor sources through a continuum or a comb spectrum have raised new opportunities to greatly simplify the implementation of STED microscopy, especially towards multicolor imaging [17,18]. Although such high peak-power pulsed laser systems make STED microscopes versatile, it has been shown that the use of continuous-wave (CW) laser sources is a technically elegant alternative, requiring no synchronization, pulse length optimization, or timing between excitation and STED beams [19].

When merging TPE with STED microscopy, the choice of laser sources is more important than in the SPE-STED case, because of the optical power requirements for both TPE and STED. Although CW-TPE has been demonstrated [20,21], (sub)picosecond NIR laser sources are the most effective for reaching the high peak-power required by TPE. From a photophysical viewpoint, nearly ideal sources for TPE-STED microscopy would be a combination of a mode-locked (sub)picosecond laser for excitation synchronized with a high peak-power visible source for STED, such as an OPO. Keeping the freedom of independently tuning the two wavelengths would require the synchronization of two modelocked systems, one for the TPE and the second for pumping the OPO. The high cost and complexity of such a combined laser system would be arguably prohibitive. In this article we demonstrate an easy way to realize TPE-STED microscopy by using a short-pulse laser for TPE and a CW laser for STED.

2. Setup

The schematic of the experimental setup is shown in Fig. 1(c). The two-photon excitation source was a compact, mode-locked diode-pumped Nd:glass femtosecond laser delivering 300 fs pulses at 1060 nm with a repetition rate of 117 MHz and an average power of 160 mW (Model GLX-200, Time-Bandwidth, Zürich, Switzerland). The beam was free-space propagated from the laser cavity to the objective lens. A telescope was used to match the beam diameter to the back aperture of the microscope objective lens (HCX PL APO 100 × /1.40–0.7 Oil, Leica Microsystems, Wetzlar, Germany) in order to obtain a diffraction limited spot for TPE. Both a half- and a quarter-waveplate were used before the dichroic mirror (725DCSP XR, AHF analysentechnik, Tübingen, Germany) to circularly polarize the excitation light at the sample, making TPE of molecules in different orientations isotropic in the focal plane.

#113468 - $15.00 USD Received 26 Jun 2009; revised 29 Jul 2009; accepted 31 Jul 2009; published 3 Aug 2009

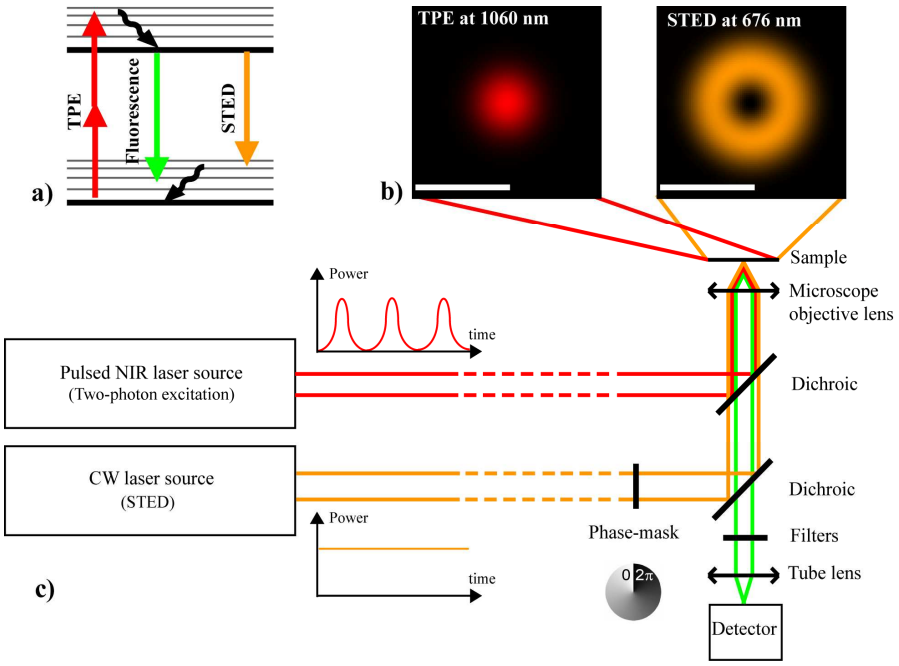

Fig. 1. Principles of the reported implementation of TPE-STED microscopy. (a) Energy diagram of the 3 processes involved. (b) Light intensity distribution of the two-photon excitation spot (left) and of the STED doughnut (right) in the focal plan. Scale bars represent 500 nm (c) Setup.

The light source for STED was a krypton CW laser providing ~1 W at 676 nm (Innova Sabre, Coherent, USA) at its output. Spatial mode cleaning of the STED beam was performed using a high-power polarization-maintaining single mode optical fiber (OZ Optics, Canada). After collimating the beam at the output of the fiber, light passed through a polymer mask imprinting a 0 to 2π helical phase-ramp (RPC Photonics, Rochester, NY, USA) in order to obtain the doughnut-like pattern at the focus. A symmetrical light distribution and zero-point intensity of less than 1.5% on the optical axis were obtained in the focal plane by imposing a circular polarization on the STED beam in the back aperture of the objective lens using an additional pair of quarter- and half-waveplates before the second dichroic (Z660SPRDC, AHF analysentechnik). Typical time-averaged optical powers used in the back aperture of the objective lens were ~7–15 mW (pulsed) and ~200 mW (CW) for the two-photon excitation and the STED beams, respectively. The associated maximum focal intensities are of the order of 200 GW/cm^2 for TPE and by three order of magnitude lower (0.2 GW/cm^2) for STED. Fluorescence light was collected by the objective lens, and passed through the dichroic mirrors and cleanup filters (E700SP and HQ600/60 or HQ560/40, AHF analysentechnik) before being focused by a 300 mm focal length doublet into a multimode fiber (62.5 µm / 0.27 NA, M31L01, Thorlabs) acting as a confocal pinhole ~0.8 times the size of the Airy disc at 600 nm. Fluorescence light was finally collected by an avalanche photodiode module (SPCM-AQR-13-FC, Perkin Elmer, Québec, Canada) connected to a photon-counting board (P7882, FAST ComTec, Oberhaching, Germany). Image acquisition was performed by scanning the sample with a 3D piezo stage (NanoBlock, Melles Griot GmbH, Bensheim, Germany). TPE-STED and TPE reference images were recorded nearly simultaneously on a line-by-line basis by opening and closing a shutter in the STED beam. All acquisition operations were automated and managed by the software Imspector.

#113468 - $15.00 USD Received 26 Jun 2009; revised 29 Jul 2009; accepted 31 Jul 2009; published 3 Aug 2009

3. Results

For testing our setup we first compared TPE and TPE-STED images of 20 nm polystyrene nanospheres containing the fluorophore Nile Red (Nile Red SPHERO, Spherotech, USA) mounted on a microscope cover glass, with poly-L-lysine as the linker and 2,2'thiodiethanol (TDE) as the embedding medium. The maxima for single-photon absorption and fluorescence emission of the fluorescent particles were 520 / 560 nm, respectively. Typical images obtained with the described setup are presented in Fig. 2. In the back aperture of the objective lens we used a time-averaged power of ~15 mW subpicosecond pulsed light for TPE at 1060 nm and ~200 mW CW power for STED at 676 nm. The pixel dwell-time was 200 µs and the pixel size 15 nm.

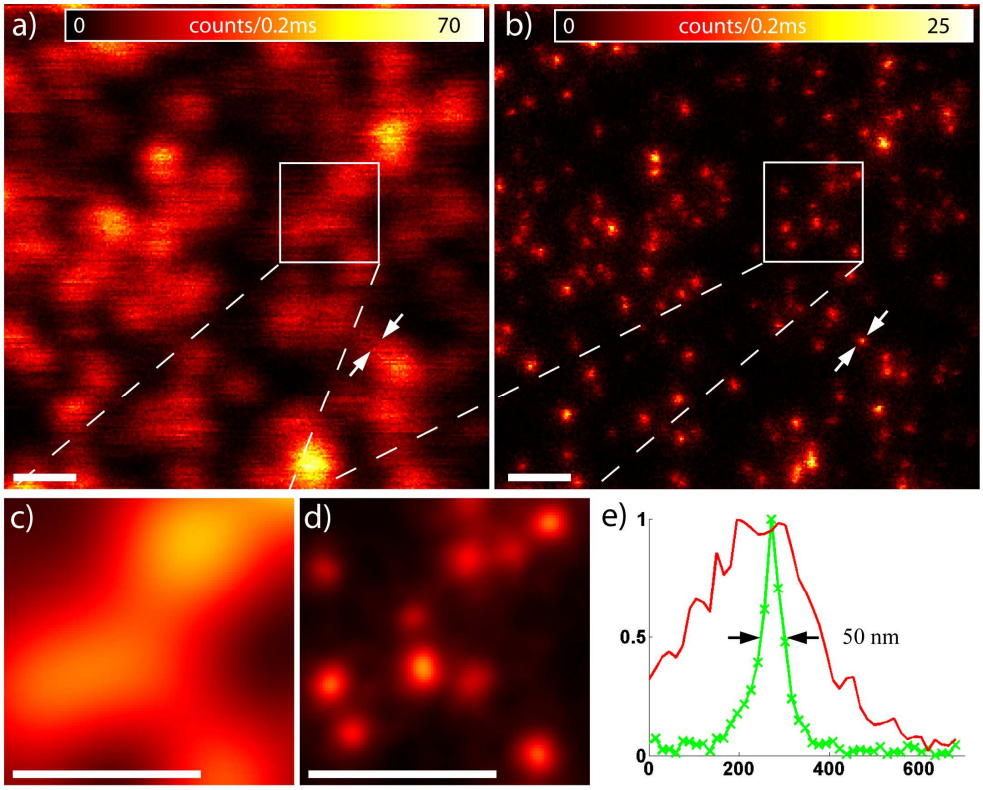

Fig. 2. Comparison of TPE and TPE-STED images of 20 nm NileRed fluorescent beads mounted on a cover glass. (a) and (b) are, respectively, the raw pictures of TPE and TPE-STED. (c) and (d) shows linearly de-convolved enlargements of the areas marked with white squares in (a) and (b). All scale bars correspond to 500 nm. Normalized line profiles taken between the arrows in (a) and (b) are plotted in (e) in red and green, respectively.

The comparison of images of the nanoparticles with TPE both with and without the presence of the STED beam clearly shows a substantial resolution enhancement. A line profile across the typical image of a single particle displays a FWHM of about 50 nm in the STED case. Considering the 20 nm diameter size of the beads, this implies an optical resolution < 50 nm in the focal plane. Taking 50 nm as an upper value this means a 5.4-fold increase in resolution over to the calculated resolution of ~270 nm offered by TPE alone, in good agreement with what can be estimated from the raw TPE picture, despite the close proximity of the beads. To increase the contrast and reduce the noise, a linear de-convolution was carried out on both pictures for fair comparison. Gaussian models with a FWHM of 50 nm and 270 nm were used for the de-convolution of TPE-STED and TPE pictures respectively

#113468 - $15.00 USD Received 26 Jun 2009; revised 29 Jul 2009; accepted 31 Jul 2009; published 3 Aug 2009

and regularization parameters were chosen such that negative values were avoided. An enlargement of a relatively dense area is shown for comparison.

Next we present transverse (xy) images of the 3D distribution of the transcription regulator NFκB in the nucleus of a mammalian PtK2 cell at different depths. NFκB was labeled with a primary antibody (polyclonal anti-NFκB p105/p50 rabbit IgG, Abcam) and stained with the dye ATTO 565 (Atto565-NHS ester, ATTOTEC GmbH, Siegen, Germany) attached to a secondary antibody (goat anti-rabbit IgG, Dianova). In order to keep the 3D structure intact, the sample was embedded in an aqueous solution of TDE following a procedure using successive steps in TDE concentration [22]. The maxima for single-photon absorption and fluorescence emission of ATTO 565 are 565 / 592 nm, respectively. For the results presented in Fig. 3, we used ~10 mW in the back aperture of the objective lens for TPE at 1060 nm and ~200 mW for STED at 676 nm. The pixel dwell-time was 200 µs and the pixel size 40 nm.

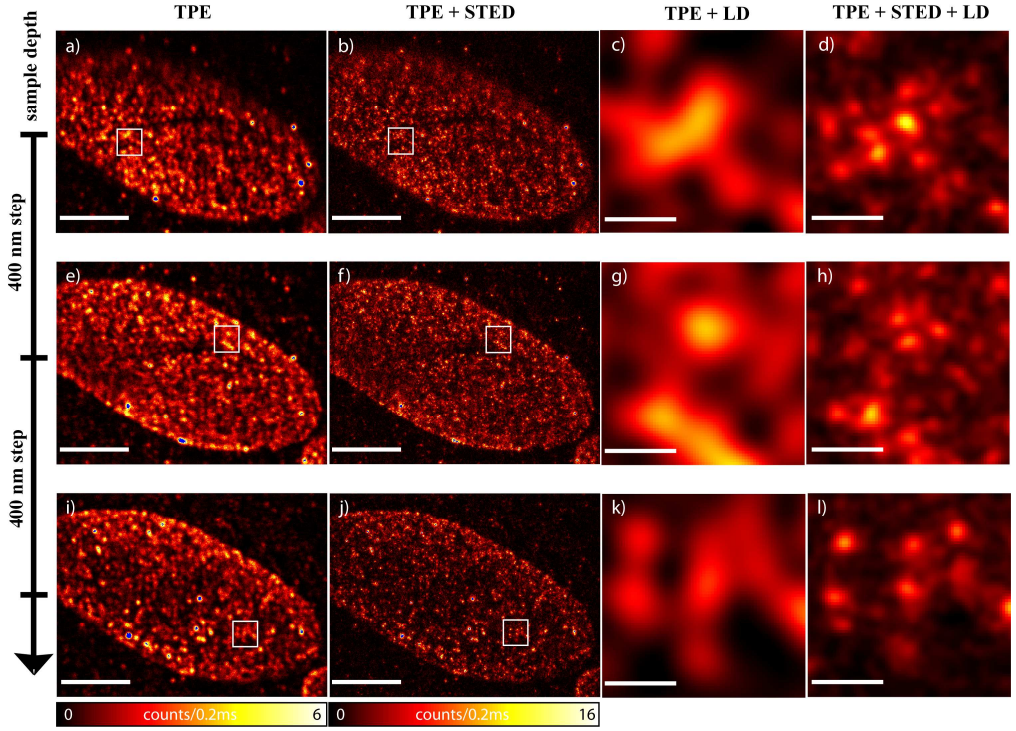

Fig. 3. Images (xy) of the 3D distribution of NFκB immunostained with ATTO 565 in the nucleus of a PtK2 cell. TPE (a,e,i) and TPE-STED (b,f,j) raw images were taken at different depths (z) along the optic axis with axial distances of 400 nm: (a,b), (e,f) and (i,j). Scale bars on these images represent 5 µm. (c) and (d) show linearly de-convolved enlargements of the areas marked with white squares respectively in (a) and (b). (g,h) correspond to (e,f), and (k,l) to (i,j). Scale bars for the zoomed in images represent 500 nm.

TPE-STED raw pictures of another cell (not shown) taken with a pixel size of 30 nm revealed smallest isolated spots with a FWHM of ~80 nm. Since the size of NFκB is negligible compared to the length of the primary and secondary antibody sandwich (~20 nm), the real size of the fluorescent structures is ~40 nm. The optical resolution in those conditions is then ~70 nm, which is about 4 times better than in TPE microscopy. This significant resolution improvement by TPE-STED over to TPE alone can also be recognized in the enlarged deconvolved images of high-density areas. Gaussian point-spread-functions with FWHM of 80 nm and 270 nm were used for the linear de-convolution of the TPE-STED and the TPE data, respectively. The regularization parameters were chosen such that negative values were avoided.

#113468 - $15.00 USD Received 26 Jun 2009; revised 29 Jul 2009; accepted 31 Jul 2009; published 3 Aug 2009

3. Discussion and conclusion

We have demonstrated the viability of a technically elegant method to combine TPE and STED microscopy for reducing the spatial confinement of the effective two-photon excitation volume. Using a short-pulse laser for TPE and a CW laser for STED a resolution < 50 nm in all directions in the focal plane has been achieved, corresponding to a 5.4-fold improvement over the diffraction limit of TPE microscopy, or a 29-fold reduction of the area of the focal spot. In the future, additional squeezing the axial extent of the excitation volume could be achieved using a second depletion pattern, as has already been reported for SPE-STED [10].

An important role is played by the ratio of the pulsed TPE and the less probable, but non-negligible, undesired fluorophore excitation caused by the CW STED beam. An increase in the repetition rate of the two-photon excitation laser would reduce this ratio in favor of the desired TPE. We therefore expect that a repetition rate higher than the 117 MHz used here would in the TPE CW-STED case not only lead to a higher TPE fluorescence signal but also offer a higher resolution at the same wavelength and power conditions for CW-STED. Alternatively, it may allow the use of a shorter STED wavelength and/or reduction of the STED power while maintaining the resolution. In this context it is interesting to note that using SPE of the same dye Atto 565, a higher resolution was achieved using less power and a shorter wavelength for STED [19].

Because it combines the advantages of TPE with the increased resolving power provided by STED, we expect TPE-STED to be useful for exploring moderately scattering and/or thick samples with subdiffraction resolution. The possible decrease of fluorescence intensity and/or resolution deep into samples needs careful attention. In this regard it is important to realize that owing to the symmetry of the helical spatial phase retardation applied to the STED beam to create the doughnut shape in the focal plane, the zero intensity in the center of the depletion pattern is not affected by spherical aberrations or other wave front distortions that are symmetrical around the optic axis. In general, the decrease of focal plane intensity I caused by aberrations reduces the resolution, but this effect can be partially counterbalanced by increasing the STED power or, more elegantly, by using adaptive optics designed to maintain the high contrast between the minimum and the doughnut crest. The only limitation TPE-STED would have over diffraction limited TPE microscopy is thus caused by scattering of the STED beam since STED light scattered into the center of the doughnut decreases the fluorescence signal. The practical relevance of these factors and thus the maximum achievable penetration depth and resolution will depend on the sample and wavelength. However, just as TPE microscopy outperforms its SPE confocal counterpart, TPE-STED should outperform confocal SPE-STED in deeper layers of a scattering sample, since scattering of the excitation and the fluorescence light is much less relevant in the TPE-STED case. Additionally, out-of-focus bleaching in TPE-STED microscopy is expected to be lower than in SPE-STED microscopy, as bleaching in STED microscopy usually involves prior excitation to the first excited singlet state which is now also limited to the focal plane.

In conclusion, we have shown that the resolution barrier in TPE microscopy can be overcome using STED. The development of new laser technologies, and in particular of high power CW solid-state laser sources, will make other combinations of fluorophores and wavelengthd usable for TPE-STED microscopy in the future.

Acknowledgments

We thank Rebecca Medda for sample preparation, Benjamin Harke for discussions about the setup, Jan Keller for discussions on image analysis, Jaydev Jethwa for his help with lasers. Andreas Schönle is thanked for his support with the software Imspector and, along with Brian Rankin, also thanked for critical reading of the manuscript.

#113468 - $15.00 USD Received 26 Jun 2009; revised 29 Jul 2009; accepted 31 Jul 2009; published 3 Aug 2009